# Debris Capture Example by Flexible Barrier and Its Performance Verification

Hiroyuki UMEZAWA[1], Risa TANABE[1*] and Peihong ZHU[1]

[1] Toa Grout Kogyo Co., Ltd., Japan (2-10-3 Yotsuya Shinjuku-ku TOKYO 160-0004 Japan)
[*]Corresponding author. E-mail:risa.tanabe@toa-g.co.jp

In recent years, sediment-related disasters occur frequently in various places. Although voluntary evacuation is being emphasized, countermeasures by structures are still important. We have developed a new type of protective barrier, which is compact and flexible, as one of the slope failure control sediment capture works. This flexible protective barrier has been installed in various locations since its first installation in 2011 and has captured debris at some of the installation sites. In this report, we will introduce examples of these debris capture cases and pick one of the examples as a sample into detailed analysis. In the detailed analysis, the validity of the existing design method was verified with reference to the slope condition after debris capture situation. The items to be verified were (1) amount of sediment captured and (2) acting force on the components. As a result, we confirmed that the existing designing method was a reasonable and safe design method.

**Key words:** debris capture, performance verification, existing designing method

## 1. INTRODUCTION

Flexibly structured slope failure control sediment capture works (hereinafter "impact barrier") is a type of works designed to control steep slope failure composed mainly of posts, wire ropes, nets, energy absorbers (hereinafter "brake ring") and underground reaction bodies (**Fig. 1**). This barrier was so far installed at 118 locations in Japan, and three of them have captured collapsed sediment successfully.

Forces in wire ropes and axial force to the post are calculated by using the static equilibrium of force based on the acting force in the net when the fence undergoes maximum deformation.

A force transmission process under impact force is shown as follows (**Fig. 2**).

(a) Impact force acts on the net.
(b) Tension is generated in the net.
(c) The tension generated in the net is transmitted to the wire ropes and posts.
(d) Forces transmitted to the wire ropes and posts are transmitted to the anchors or underground reaction bodies.

Size of cross section surfaces for each component is designed by using the allowable stress intensity method based on these forces (hereinafter the "existing design method"). The barrier is verified in a full-size experiment by validating the viability of its constituent factors including the safety factor of each component and the force equilibrium.

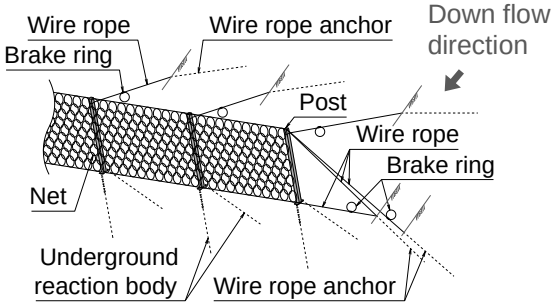


**Fig. 1** Schematic diagram of structure

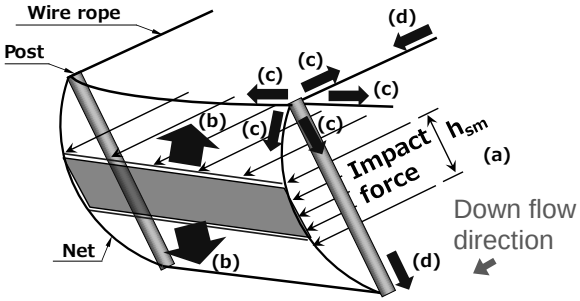


**Fig. 2** Design model (under impact force)

**Fig. 3** Deformation of ring net - (left) unloaded, (right) loaded

**Fig. 4** Deformation of brake ring - (left) unloaded, (right) loaded

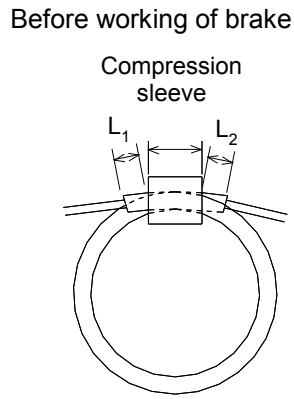


**Fig. 5** Conceptual diagram of brake ring travel (before working)

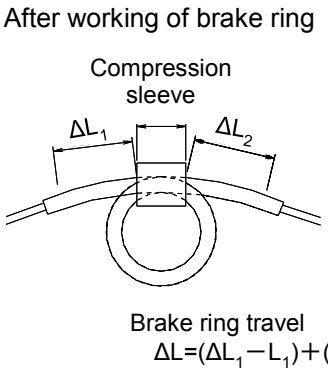


**Fig. 6** Conceptual diagram of brake ring travel (after working)

This paper reports the verification result of the validity of the design with (1) amount of sediment captured and (2) acting force on the components used as focal points while using actual sediment capture data.

**Table 1** Outline of collapsed sediment capture cases

| Case | | (a) | (b) | (c) | (d) |
|---|---|---|---|---|---|
| Construction site | | Miyazaki | | Hyogo | Shizuoka |
| Construction completed year | | 2011 | | 2013 | 2014 |
| Sediment captured year | | 2011 | 2012 | 2014 | Around 2016 |
| Fence height | | 5.0 m | | 4.0 m | 5.5 m |
| Fence length | | 20 m | | 120 m | 24 m |
| Impact force of the failed sediment | Design conditions 1) | 135.9 kN/m$^2$ | | 135.7 kN/m$^2$ | 108.9 kN/m$^2$ |
| | Estimation 2) | 87.7 kN/m$^2$ | 120.7 kN/m$^2$ | 41.5 kN/m$^2$ | - |
| | 3) = 2) / 1) | 0.65 | 0.89 | 0.31 | - |
| Estimator of sediment capture | | 40 m$^3$ | 360 m$^3$ | 450 m$^3$ | 55 m$^3$ |
| Effective fence height (deposit height) | Design conditions | 4.5 m | | 3.45 m | 5.0 m |
| | Estimation | (2.0 m) | (4.5 m) | (2.5 m) | (1.7 m) |

## 2. Main energy absorbing components of Impact barrier

The main energy absorbing components of impact barrier are ring net and brake ring.

The net is knitted with rings, which are consist of high-tensile steel wire and bundled into a circular shape with a diameter of 30 cm. Each ring is connected to another ring at 4 points. When a load acts on the net, a ring is extended and deformed from a circle to quadrangle and absorbs the energy (**Fig. 3**). Because of its flexible character, it is utilized for capturing various objects such as falling rocks, debris flow, driftwood and high-speed flying objects besides collapsed sediment.

The brake ring, an energy absorber consists of steel tube, which is bent into a loop and a wire rope is guided through this steel tube. The end of steel tube is held by compression sleeve. When a tension above a certain level acts on the wire rope, the steel tube is deformed to narrow down and defuses the working load, reduce the acting force on the wire rope (**Fig. 4, 5,** and **6**). It is a major feature, even if the brake ring is transformed, the wire rope is not damaged by friction.

In addition, in order to capture the collapsed sediments safely by impact barrier, replacement criteria are set up for components that allow


**Fig. 7** Capture case of collapsed sediment (a)


**Fig. 8** Capture case of collapsed sediment (b)

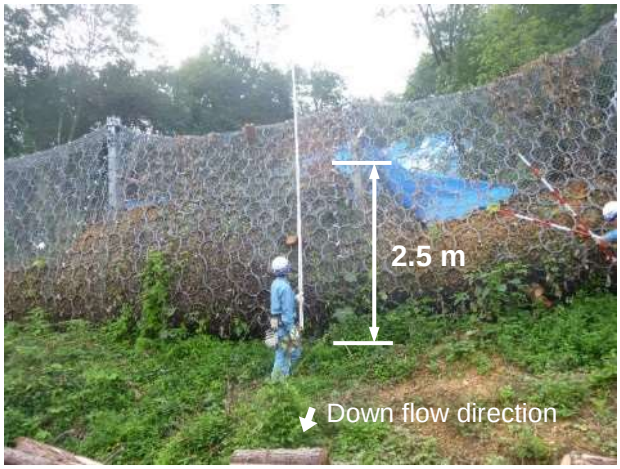


**Fig. 9** Capture case of collapsed sediment (c)


**Fig. 10** Capture case of collapsed sediment (d)

deformation. For example, in the case of ring net, replacement is performed, when the wire of ring is greatly plastically deformed or fractured. In the case of brake ring, replacement is performed, when the travel of brake ring exceeds 40cm (**Fig. 5** and **6**).

## 3. Outline of collapsed sediment capture cases

So far impact barriers have collected a record of capturing collapsed sediment in three locations. One of the impact barriers has captured collapsed sediment twice. An outline of collapsed sediment capture cases is shown in **Table 1**. Case (a) and Case (b) were captured by the same impact barrier. The capture situation of collapsed sediment in each case is shown in **Fig. 7, 8, 9** and **10**.

### 3.1 Capture case of collapsed sediment (a)

The impact barrier of case (a) was installed for road damage restoration work conducted in Miyazaki prefecture in 2011. This impact barrier has a 20 m long and 5 m high fence. In 2011, small slope failure occurred and the barrier captured about 40 $m^3$ of collapsed sediment (**Fig. 7**). The impact force acting on the barrier estimated from the slope collapse situation was 87.7 $kN/m^2$, which was about 65% of the design condition of 135.9 $kN/m^2$.

Since deformation and damage of the components were not observed, the barrier remained to be used after the removal of the sediment without any replace of the components.

### 3.2 Capture case of collapsed sediment (b)

Case (b) is a case of capturing collapsed sediment again the year after case (a). When the upper part of the slope, at the foot of which this barrier was constructed, failed as a result of heavy rainfall in July 2012, the barrier captured about 360 $m^3$ sediment that collapsed from the slope (**Fig. 8**). The estimated impact force acting on the barrier was 120.7 $kN/m^2$, which was about 89% of the design condition of 135.9 $kN/m^2$. Since deformation exceeding the replacement criteria was seen in ring nets and brake rings on the retaining ropes, replaces of components were carried out to restore the performance after the removal of the sediment.

### 3.3 Capture case of collapsed sediment (c)

The impact barrier of case (c) was applied to the steep slope failure prevention project in Hyogo prefecture in 2013.The installation length was long (about 240m). The design external force and the sediment capture capacity of the barrier of each slope were different. Considering these conditions and the ease of land use, the barrier was divided into 3 fences. The fence that captured the collapsed sediment is 120m long and 4m high.

In 2014, the impact barrier captured about 450 $m^3$ of collapsed sediment caused by Typhoon No.11 (**Fig. 9**). The estimated impact force acting on the barrier was 41.5 $kN/m^2$, which was about 31% of the design condition of 135.7 $kN/m^2$.

Although deformation of the ring net around the post head in the sediment capturing part was observed, it was not such an extent of deformation or damage of components as to hinder the performance. After removing the sediment, since deflection was observed in the support rope, which is a net suspension rope, it was re-tensioned. And the wire mesh, which is installed on the mountain side of ring net and prevents the passage of small sized soil, was damaged in the sediment capturing part, so it was replaced to restore the initial performance at the time of installation.

### 3.4 Capture case of collapsed sediment (d)

Impact barrier in case (d) was installed also for road damage restoration work in Shizuoka prefecture in 2014. The timing of the occurrence of collapse sediment was not clear, while impact barrier had captured about 55 $m^3$ of the collapsed sediment was confirmed during the field survey conducted in 2016 (**Fig. 10**). In this site, since the slope situation after collapse was considered to be dangerous, we had not confirmed the slope collapse situation.

Since deformation and damage of the components were not observed, the barrier remains being used after the removal of the sediment without any replace of the components.

### 3.5 Capture case for performance verification

For impact barrier, replacement criteria are set for each component, and when the amount of deformation of the component exceeds the standard, it has to be replaced. Therefore, we choose case (b), where the estimated impact force was closest to the design condition and the components deformation exceeding the replacement criteria were observed, to be the performance verification study case.


**Fig. 11** Works completed


**Fig. 12** Sediment deposit height

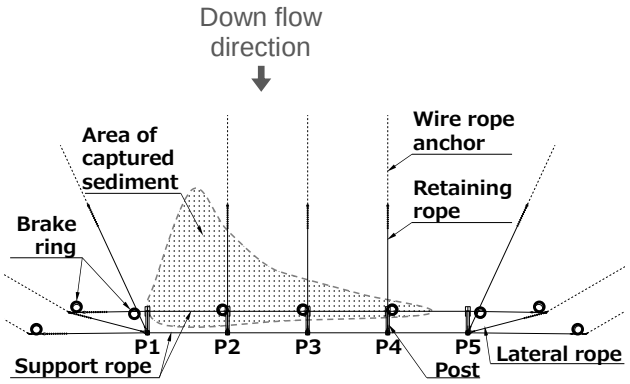


**Fig. 13** Capture of sediment (plan view)

## 4. Details of collapsed sediment capture situation of case (b) subject to performance verification

The barrier when completed is shown in **Fig. 11** and the barrier when it captured the sediment is shown in **Fig. 8, 12, 13**. The design conditions and the field slope failure conditions confirmed by the follow-up survey are shown in **Table 2** and schematic sectional diagrams of the fence in its design condition

**Table 2** Design conditions and the estimation based on actual capture of sediment

| Item | Sign | Design conditions | Estimation based on actual capture of sediment | Ratio to the design conditions |
|---|---|---|---|---|
| | | 1) | 2) | (3) = 2) / 1) |
| Impact force of the failed sediment | $F_{sm}$ | 135.9 kN/m$^2$ | 120.7 kN/m$^2$ | 0.89 |
| Deposited earth pressure of the failed sediment | $F_{sa}$ | 19.8 kN/m$^2$ | 24.1 kN/m$^2$ | 1.22 |
| Amount of sediment captured | V | 312 m$^3$ | 360 m$^3$ | 1.15 |

**Table 3** Design and slope failure site conditions

| Item | Sign | Design conditions | Actual phenome-non |
|---|---|---|---|
| Slope height | H | 92.69 m | 106.9 m |
| Maximum failure depth | D | 2.0 m | 1.5 m |
| Height of sediment movement | $h_{sm}$ | 1.0 m | 0.75 m |
| Slope gradient | θ | 35° | 37° |
| Internal friction angle | φ | 35° | 30° |
| Effective fence height (deposit height) | h | 4.5 m | (4.5 m) |

and in the condition when it captured the sediment is shown in **Fig. 14, 15**. The maximum failure depth estimated from the ground surface line before and after the slope failure is about 1.5 m (**Fig. 16**).

## 5. Comparison Between Follow-up Survey Results and Calculated Value of the Existing Design Method

### 5.1 Comparison of acting forces on the impact barrier

The design conditions and the impact force that worked on the impact barrier upon capture of the sediment and the deposited earth pressure are shown in **Table 3**. For the force that worked on the impact barrier when the sediment was captured, the slope failure conditions were considered (**Fig. 12, 13 14, 15, 16**), and the impact force and deposited earth

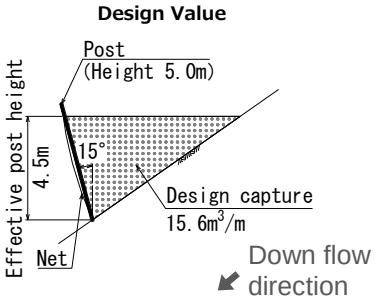


**Fig. 14** Schematic sectional diagrams of the fence in the design condition

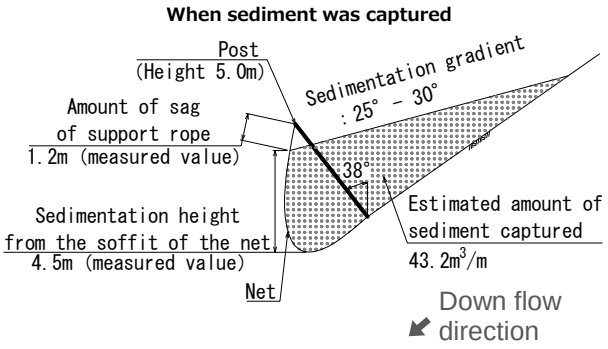


**Fig. 15** Schematic sectional diagrams of the fence in the sediment capture condition

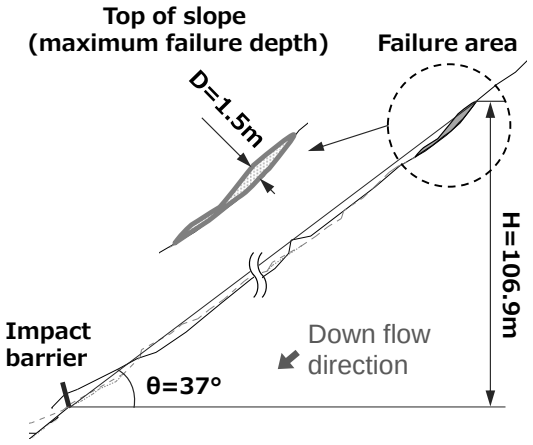


**Fig. 16** Condition of collapse at the slope failure site

pressure were calculated using the calculation equation specified by MLIT Notification No. 332 (March 28, 2001). The calculation results indicate an impact force smaller by about 10% than the design value and a deposited earth pressure, calculated from the sediment deposition height at the site that was larger by about 22% than the design value. This is due to the difference in internal friction angle. Although the internal friction angle was set to 35 ° under design conditions, in the actual phenomenon, it was set to 30 ° with reference to the sediment gradient of the sediment deposited inside the impact barrier.

One of the factors that made the impact force at the time of sediment capture come out smaller than


**Fig. 17** Measuring the reading of the brake ring travel

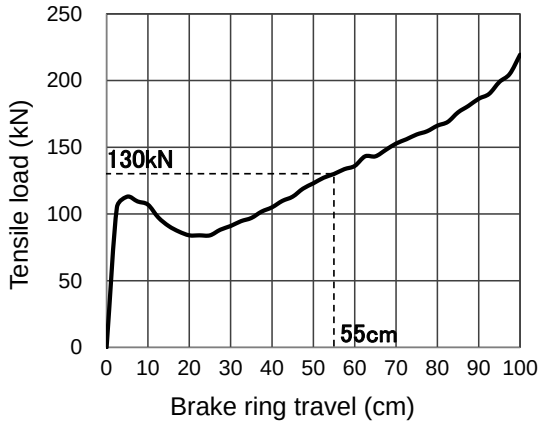


**Fig. 18** Relationship between the loading and travel of the brake ring

the one determined by the design conditions is that the actual maximum failure depth (D) was smaller than the one determined by the design conditions.

### 5.2 Comparison of the amount of sediment captured

The impact barrier is a structure that tolerates large deformations under the impact of the failed sediment. When the effective fence height is determined according to the existing design method, the deformation of the net and slanting of the posts are considered based on the full-size experiment so that the predetermined amount of sediment can be captured even after the fence is deformed by capturing the failed sediment. The amount of sediment captured by the subject impact barrier is 360.9 $m^3$ according to the calculation using the reference data of the survey longitudinal profile and plan view after the slope failure. When compared with the design capture (312 $m^3$), the actual capture was about 15% greater.

The maximum amount of capture by the unit width is 43.2 $m^3/m$ according to the calculation based on the survey longitudinal profile, which is about 180% larger than the design value (15.6 $m^3/m$). The actual values turned out to be considerably larger than the design values because the design conditions allow for no sedimentation gradient, the actual sedimentation gradient at the failure site was 25˚ to 30˚, and sediment was intensively deposited because of the valley topography.

**Table 4** Estimate of force acting on the retaining rope and the margin of the existing design method

| Estimate based on the brake ring travel | Acting force based on the existing design method | Margin of the existing design method |
|---|---|---|
| 4) | 5) | 6) = 5) / 4) |
| 260.0 kN | 280.8 kN | 1.08 |

## 6. Comparison of force acting on wire ropes

For the force acting on components, 1) the estimate made from the brake ring travel based on the survey result was compared with 2) the force acting on the rope calculated from the existing design method based on the slope conditions at the subject site, with respect to the retaining ropes, which are the mountainside stay ropes on the post.

### 6.1 Estimation of the acting force on the wire rope based on the measurement of the brake ring travel

The force acting on the wire rope based on the survey result was estimated from the travel of the brake ring connected to the wire rope (**Fig. 5, 6, 17**) and the load and travel relational curve in the static material tensile test (**Fig. 18**).

At the subject failure site, sediment deposited mainly among the left-end posts, or from P1 to P3 (**Fig. 13**). Considering this, the retaining rope on the P2 post is used for comparison. The measured travel of the brake ring is 55 cm. Considering this and based on **Fig. 18**, a load of about 130 kN is considered to have worked. Since two retaining ropes were connected to the P2 post, the force acting on the ropes is estimated to be 260 kN (130 kN × 2).

### 6.2 Estimation of the force acting on the wire rope based on the existing design method

The maximum force acting on the retaining rope based on the existing design method is 280.8 kN, with the slope failure condition at the failure site (**Fig. 12, 13 14, 15, 16**) taken into consideration. The retaining rope acting force based on the existing design method turned out to be about 8% larger than the acting force estimated from the brake ring travel. The estimate of force acting on the retaining rope and the margin of the existing design method are shown in **Table 4**.

## 7. COMPONENT DEFORMATION

The deformation of the net, post head and post base after capturing sediment are shown in **Fig. 19, 20,** and **21**. Deformation that may affect sediment capture performance was not confirmed at any component.

## 8. CONCLUSIONS

The amount of sediment captured and the force acting on the wire rope were verified base on the condition of the slope after failure and the condition of the captured sediment. The impact barrier chosen as the subject of verification is a structure that satisfies the three conditions required of a sediment capture works for steep slope failure control. To be specific, this structure is (1) a structure that satisfies the conditions specified by MLIT Notification No. 332, (2) a structure that resists the predetermined deposited earth pressure, and (3) a structure that can maintain the predetermined amount of sediment to be captured. In addition, the existing design method is confirmed a reasonable and safe design method.

We have identified some tasks to solve in the future. To be specific, we will need to conduct a dynamic material tensile test for the brake ring and understand the relationship with the load and travel in order to ensure a precise evaluation of acting force under the impact of a collapsed sediment. We will also need to conduct more follow-up surveys and enhance the reliability for validity of the design method by the verification method used herein.


**Fig. 19** Deformation of the ring net


**Fig. 20** Deformation of the post head


**Fig. 21** Deformation of the base plate

**REFERENCES**

Chiba, M., Sakaguchi, T., Shimojo, K., Imura, T. and Buginion, L. (2011): Effect of flexible protection barriers on slope failure, Journal of the Japan Society of Erosion Control Engineering, Vol. 64, No. 1, pp. 25-29

MLIT Notification No. 332 (2001): Notification on the methods specified by the Minister of Land, Infrastructure, Transport and Tourism as per the provision of Item 2, Article 2, Enforcement Order for the Law related to Promotion of Measures for Sediment-related Disaster Area etc. due to Sediment-related Disaster (March 28, 2001)

Musashi, Y., Kimura, Y., Umezawa, H. and Mizuyama, T. (2014): Distinct Element Simulation on the Process of Impact Force Absorption of the Flexibly Structured Sediment Capture Works, FY2014 JSECE Research Presentation Compendium, pp. B-248-B-249

Sabo & Landslide Technical Center (2011): Construction Technology Examination Certificate (Sabo Technology) Report "Impact Barrier Method"